ACCSCIENCE PUBLISHING

Eurasian Journal of Medicine and Oncology

ORIGINAL RESEARCH ARTICLE

Mechanism of isorhamnetin in treating triple-negative breast cancer based on network pharmacology, molecular docking, and in vitro verification

Yanan Hua[1,2]*, Xiangyu Xie[1], Li Sun[1], Enqi Liu[1], and Shuqi Niu[1,2]*

[1]Department of Biology, College of Medical Technology, Chengdu University of Traditional Chinese Medicine, Chengdu, Sichuan, China

[2]Chongqing Key Laboratory of Sichuan-Chongqing Co-construction for Diagnosis and Treatment of Infectious Diseases Integrated Traditional Chinese and Western Medicine, Chengdu University of Traditional Chinese Medicine, Chengdu, Sichuan, China

Abstract

Introduction: Triple-negative breast cancer (TNBC) is a highly aggressive subtype of breast cancer with poor prognosis and limited targeted therapies. The development of novel effective drugs is of great significance for TNBC treatment.

Objective: This study aims to clarify the molecular mechanisms through which isorhamnetin(ISO) restrains the malignant progression of TNBC, usingcomputational pharmacology prediction and empirical verification.

Methods: We systematically screened public online databases and identified 198 putative targets of isorhamnetin and 1,490 genes functionally associated with TNBC. Overlapping targets were obtained through Venn diagram analysis. By integrating protein–protein interaction network profiling, functional enrichment analysis, and molecular docking experiments, we predicted the key binding targets of isorhamnetin. We then validated the effects of isorhamnetin on cell proliferation, migration, and invasion in TNBC cell lines. Western blot and cellular thermal shift assays were employed to examine target protein expression and alterations in downstream signaling pathways.

Results: The combination of protein–protein interaction network profiling, functional enrichment analysis, and molecular docking experiments indicated that ISO binds epidermal growth factor receptor (EGFR) with high affinity. Our findings revealed that ISO strongly reduced the growth, motility, and infiltrative capacities of TNBC cells. Western blot and cellular thermal shift assays confirmed that ISO downregulates EGFR protein expression and modulates downstream mammalian target of rapamycin (mTOR) and MAPK/ERK kinase (MEK)/extracellular signal-regulated kinase (ERK) signaling.

Conclusion: ISO suppresses TNBC progression by downregulating EGFR signaling, providing a theoretical basis for its clinical application.

Keywords: Isorhamnetin; Triple-negative breast cancer; Epidermal growth factor receptor; Network pharmacology; Molecular docking

***Corresponding authors:**
Yanan Hua
(huayanan@cdutcm.edu.cn)
Shuqi Niu
(niushuqi@cdutcm.edu.cn)

Citation: Hua Y, Xie X, Sun L, Liu E, Niu S. Mechanism of isorhamnetin in treating triple-negative breast cancer based on network pharmacology, molecular docking, and in vitro verification. *Eurasian J Med Oncol.* doi: 10.36922/EJMO026070076

Received: February 9, 2026

Revised: May 8, 2026

Accepted: May 15, 2026

Published online: July 14, 2026

1. Introduction

Among women, breast cancer presents distinctive epidemiological features and marked heterogeneity, making it a leading contributor to cancer-related death.[1] Triple-negative breast cancer (TNBC), characterized by high invasiveness and metastatic potential, has a significantly higher fatality rate compared with other molecular subtypes. Metastasis is the primary cause of death in TNBC patients.[2,3] Current treatment strategies for TNBC mainly rely on chemotherapy and immunotherapy, yet fewer than 20% of patients benefit from these regimens.[4] Therefore, developing novel, safe, and effective therapeutic approaches is imperative to improve the prognosis of breast cancer patients.

Traditional Chinese medicine offers distinct advantages and broad application prospects in cancer treatment.[5] Its ability to act on multiple molecular targets and biological pathways provides a useful framework for holistic cancer management.[6] Currently, research on traditional Chinese medicine for breast cancer is increasing and has demonstrated notable benefits, particularly in alleviating adverse reactions associated with radiotherapy and chemotherapy. Natural products such as terpenoids, alkaloids, and flavonoids have become hotspots in preclinical breast cancer research due to their abundant sources, significant efficacy, and low toxicity.[7-9] Flavonoids have attracted considerable attention for their broad-spectrum anti-tumor activity,[10] including inhibition of tumor cell proliferation, promotion of apoptosis, modulation of signaling pathways, reduction of invasion and metastasis, and suppression of angiogenesis. For example, icariin induces G0/G1 phase cell cycle arrest and promotes apoptosis by downregulating cyclin D1, cyclin-dependent kinase 2 (CDK2), and CDK4 expression.[11] By suppressing nuclear factor-kappa B (NF-κB) signaling, anthocyanins reduce the proliferative and invasive capacities of breast cancer cells.[12] Grape seed proanthocyanidins reduce tumor angiogenesis by inhibiting vasculogenic mimicry in HCC1937 cells,[13] whereas cardamonin induces breast cancer cell apoptosis by modulating B-cell lymphoma 2 (BCL-2), BCL-a2-associated X protein (BAX), cytochrome c (Cyt-C), poly(ADP-ribose) polymerase (PARP), and cleaved caspase-3.[14] Further exploration of the anti-tumor mechanisms of flavonoids and optimization of their clinical application strategies will help promote the broader use of traditional Chinese medicine in cancer treatment and provide patients with more therapeutic options.

Isorhamnetin (ISO) is a flavonoid derivative widely found in medicinal plants and possesses extensive pharmacological activities. Its anti-tumor effects have garnered increasing attention. Studies indicate that ISO can inhibit tumor progression in various cancer models, including liver, bladder, and lung cancers, through mechanisms such as activation of apoptosis, repression of epithelial–mesenchymal transition, and modulation of metabolic reprogramming.[15-17] Its mechanisms are cancer-type-specific: in malignant bladder cells, it mediates apoptosis by activating the AMP-activated protein kinase (AMPK)/mammalian target of rapamycin (mTOR) signaling pathway, whereas in lung cancer models, it blocks epithelial–mesenchymal transition by inhibiting the Akt/extracellular signal-regulated kinase (ERK)1/2 signaling axis, thereby reducing tumor aggressiveness.[18,19] However, research on the mechanisms of ISO in breast cancer remains insufficient, particularly regarding its relationship with key angiogenesis-related signaling pathways such as the hypoxia-inducible factor 1 alpha (HIF-1α)–vascular endothelial growth factor A (VEGFA) axis, which represents an important direction for future studies.

As a member of the growth factor receptor family, epidermal growth factor receptor (EGFR) participates in cell proliferation and signaling. It predominantly localizes to the surface of mammalian cells. When its structure or expression becomes abnormal, it may result in uncontrolled cell proliferation and differentiation.[20] Abnormal binding of EGFR with its ligands promotes homo- or heterodimerization, resulting in phosphorylation of the receptor tyrosine kinase domain. This, in turn, drives abnormal cell proliferation, promoting tumorigenesis and metastasis.[21] Studies have shown that smoking-mediated EGFR alterations correlate with an elevated risk of non-small cell lung cancer (NSCLC).[22] In NSCLC, colorectal cancer, and other malignancies, EGFR is regarded as a critical therapeutic target.[23] In colorectal cancer, cetuximab-mediated EGFR inhibition can effectively disrupt EGFR-driven signaling pathways and suppress cancer cell proliferation.[24] In head and neck squamous cell carcinoma, EGFR-targeted therapeutic strategies have also received clinical approval. According to existing reports, the initiation and progression of TNBC are likewise associated with EGFR dysregulation.[25] Aberrant levels of certain transcriptional regulators and metabolic compounds can increase EGFR expression and promote phosphorylation of EGFR and its downstream signaling proteins, thereby promoting breast cancer progression. TNBC-related studies suggest that specific transcription factors, metabolites, plant extracts, and other substances can modulate EGFR, inhibit its expression, block downstream signaling, and thereby suppress tumor cell proliferation, migration, and invasion, making EGFR an important target for precision therapy in TNBC.[26,27] Preliminary data suggest that ISO may inhibit TNBC progression by targeting EGFR. This study aims to elucidate

its molecular mechanisms through molecular docking, cellular thermal shift analysis, and functional experiments. These findings are expected to provide a theoretical framework for further research on ISO in breast cancer treatment and pharmacological insights for developing natural small-molecule therapies for breast cancer.

2. Materials and methods

2.1. Screening of potential targets of isorhamnetin

The structural file of ISO was obtained from the Traditional Chinese Medicine Systems Pharmacology Database and Analysis Platform (TCMSP) database and submitted to the SwissTarget Prediction (http://www.swisstargetprediction.ch/) and SuperPred (https://prediction.charite.de/) databases. Targets were filtered based on a prediction probability greater than 0. Standardization of gene names and removal of duplicates were performed using the Uniprot database, and the integrated set of potential targets was obtained.

2.2. Collection of triple-negative breast cancer-related targets

Target genes related to TNBC were collected from three human disease databases through a search using "Triple-Negative Breast Cancer"; the results are shown below:

(i) GeneCards (https://www.genecards.org/): All associated genes were retrieved and filtered according to the Relevance Score; genes with a score ≥10 were selected as high-confidence TNBC-related targets.
(ii) OMIM (https://omim.org/): Entries related to TNBC were searched, and genes annotated as "Triple-Negative Breast Cancer" or associated with its clinical phenotypes were collected.
(iii) DisGeNET (https://www.disgenet.org/): Retrieved targets were filtered to include those derived from genome-wide association study (GWAS), text mining, and animal model studies, retaining genes with a gene-disease association score (GDA score) ≥0.1.

The target gene lists obtained from the three databases were consolidated, and duplicates were removed using Excel (Microsoft, United States [US]) or the UNIQUE function in R. The resulting deduplicated set of TNBC-related targets was used for subsequent intersection analysis with ISO targets.

2.3. Acquisition of common targets of isorhamnetin and triple-negative breast cancer

The potential target set of ISO (198 targets) obtained through database prediction and the TNBC-associated target set (1,490 targets) collected from disease databases were compiled into lists of gene symbols. Both gene lists were uploaded to the Venny 2.1 web-based tool for Venn diagram generation (https://bioinfogp.cnb.csic.es/tools/venny/). After selecting the "Submit" function, the intersecting portion of the resulting diagram indicated the shared entries across the two collections. The analysis identified 61 common targets between ISO and TNBC (Figure 1). These common targets were considered potential key targets through which ISO may exert therapeutic effects against TNBC and were subsequently used for protein–protein interaction network analysis and functional annotation analysis.

2.4. Protein interactome construction and key target identification

The overlapping targets were uploaded to the STRING platform to obtain protein–protein interaction data, and the resulting dataset was then loaded into Cytoscape 3.10.3 to construct the protein–protein interaction network. The Centiscape 2.2 plugin was used for key gene analysis. Core targets were screened based on three parameters: degree, closeness, and betweenness. Finally, a core target diagram was generated according to degree values.

2.5. Gene Ontology and Kyoto Encyclopedia of Genes and Genomes enrichment analyses

The DAVID online analysis platform was used for bioinformatics analysis of the common targets. Across the three core Gene Ontology (GO) domains—biological process, cellular component, and molecular function—GO annotation analysis was performed. Kyoto Encyclopedia of Genes and Genomes (KEGG) pathway overrepresentation analysis was used to identify the 20 most statistically significant pathways. Data were processed using the Microbioinfo platform, and bubble plots were generated for visualization.

2.6. Molecular docking

The three-dimensional Structure Data File (SDF) structure of ISO was obtained from the PubChem repository (https://pubchem.ncbi.nlm.gov/) and converted to MOL2 format using OpenBabel 2.3.2. AutoDockTools was then used to prepare the ligand by adding hydrogen atoms, calculating partial charges, designating atom types, and generating a PDBQT file for docking. Crystal structures of the core targets were downloaded from the Protein Data Bank (PDB). Selection criteria included a resolution better than 2.5 Å, no co-crystallized ligands or mutations, and human origin. The PDB structures were preprocessed with AutoDockTools by removing water molecules, adding polar hydrogens, calculating Kollman charges, and converting the receptors to PDBQT format. Molecular docking was

performed using AutoDock Vina version 1.1.2. Binding affinities were visualized as a heatmap using Seaborn (Python) or GraphPad Prism (version 10.1.2, GraphPad Software, US). Interaction modes between the ligand and target proteins were visualized and analyzed using PyMOL, and the key interaction diagrams were saved.

2.7. Cellular thermal shift assay

Two 100 mm culture dishes were each seeded with logarithmically growing human mammary carcinoma cell lines MDA-MB-231 and MDA-MB-468. The cells were then transferred to a 37 °C incubator with 5% CO_2. After they reached approximately 80% confluence, one dish received ISO at a final concentration of 40 μmol/L (treatment group), whereas the other dish received an equivalent amount of dimethyl sulfoxide (DMSO; vehicle control). After incubation for the appropriate duration, the culture medium was removed, and the cell layer was rinsed twice with chilled phosphate-buffered saline (PBS). Next, the cells were detached with 0.25% trypsin–ethylenediaminetetraacetic acid (EDTA), and the enzymatic reaction was stopped by adding serum-supplemented complete medium. The cell suspension was collected and centrifuged at 4 °C for 5 min at 1,000 rpm. The supernatant was discarded, and the pellet was resuspended in ice-cold PBS, counted, and diluted to a density of approximately 1×10^7 cells/mL.

Each cell suspension was divided into seven aliquots of 50 μL and subjected to seven temperature gradients: 40 °C, 43 °C, 46 °C, 49 °C, 52 °C, 55 °C, and 58 °C (the MDA-MB-231 cell line was subjected to the above temperature gradient, while the MDA-MB-468 cell line was treated at temperatures 3 °C higher than the corresponding points for MDA-MB-231). Heating was performed using a polymerase chain reaction (PCR) instrument, with each temperature maintained for 3 min at a ramp rate of 1 °C/s. After heating, the samples were immediately cooled on ice for 1 min and then frozen overnight at −80 °C.

The next day, the cryopreserved pellets were warmed to ambient temperature, and an equal volume of cell lysis buffer supplemented with protease and phosphatase inhibitors was added. The cells were then lysed on ice for 15 min, after which the mixture was centrifuged at 12,000 rpm for another 15 min at 4 °C. After centrifugation, the clear supernatant was collected, and the total protein in each sample was assessed using the bicinchoninic acid (BCA) method. Equal amounts of protein from each sample were resolved by sodium dodecyl sulfate–polyacrylamide gel electrophoresis (SDS-PAGE), transferred to polyvinylidene fluoride (PVDF) membranes, and blocked with 5% non-fat milk for 1 h. The membranes were then incubated overnight at 4 °C with the primary antibody, such as anti-EGFR (A23381, Abclonal, China), and subsequently incubated with species-specific secondary antibodies for 1 h at room temperature (goat anti-rabbit IgG H&L; 511203, Zenbio, China). Protein bands were visualized with enhanced chemiluminescence (ECL; SQ201, Epizyme, China). The thermal stability of EGFR after ISO treatment was assessed by comparing the remaining target protein at different temperatures with that in unheated controls or a reference protein.

2.8. Cell counting kit-8 assay for cell viability

Cells in the logarithmic growth phase were washed with PBS, digested with trypsin, and centrifuged to collect the pellet, which was then resuspended in complete medium. The cells were seeded into 96-well plates at a density of 3,000 cells per well. After incubation at 37 °C with 5% CO_2 for 24 h, the medium was replaced with fresh medium containing ISO (0, 10, 20, or 40 μM). After another 24 h of incubation, the cells were washed with PBS, and complete medium containing 1% cell counting kit-8 (CCK-8) was added and incubated for 1 h. Absorbance at 450 nm was measured using a microplate reader (Synergy HTX, BioTek, US).

2.9. Colony formation assay

Triple-negative breast cancer cells in the logarithmic growth phase were digested with trypsin, centrifuged, and resuspended in complete medium. After counting, the cells were seeded into 6-well plates at a density of 2,000 cells per well and incubated at 37 °C with 5% CO_2 for 24 h. The cells were then treated with ISO (0, 10, 20, or 40 μM) for 48 h, after which the medium was replaced with complete medium. Cultivation continued for up to 14 days, with medium changes every 3 days, until most colonies contained more than 50 cells. The plates were photographed. After rinsing with PBS, the cells were fixed in 4% paraformaldehyde for 30 min and stained with crystal violet for 10–20 min. Following another PBS wash, the colonies were air-dried before images were captured for documentation using a microscope (DMIL LED, Leica, Germany).

2.10. Wound healing assay

Logarithmically growing MDA-MB-231 cells were dissociated with trypsin, and the samples were centrifuged at 1,000 rpm for 5 min to obtain a pellet. The cells were resuspended and counted. Subsequently, the cells were plated into 6-well plates at a density of 1×10^5 cells per well, with each well receiving 2 mL of complete medium, and incubated at 37 °C in 5% CO_2 for 24 h until they reached 90–95% confluence. Using a sterile 200 μL pipette tip,

a linear wound was made across the center of each well, with a ruler positioned at a right angle. After scratching, the wells were gently washed three times with PBS to remove detached cells. Then, 2 mL of serum-free medium containing different concentrations of ISO (0, 10, 20, or 40 μM) was added to each well.

Immediately after scratching (0 h), images of the wounds were captured under an inverted microscope at fixed positions for each well. Incubation was then continued for another 48 h. At 48 h, images were again captured at the same positions. Using ImageJ software (National Institutes of Health, US) (or a comparable image analysis tool), the wound area or width was quantified, and the percentage of wound closure was determined.

2.11. Transwell assay

A volume of 100 μL of complete culture medium was added to Transwell inserts positioned in 24-well plates, followed by a 1-h pre-incubation at 37 °C with 5% CO_2. After the initial incubation, the inserts were transferred into wells containing 600 μL of complete growth medium supplemented with 20% fetal bovine serum (FBS). After 48 h of drug treatment, the cells were collected, washed with PBS, detached with trypsin, and resuspended in serum-free Dulbecco's modified Eagle medium (DMEM). The cell suspension was adjusted to 2×10^4 cells per 100 μL, and this mixture was added to the upper chamber of the Transwell device. After 6 h of incubation under standard culture conditions (37 °C, 5% CO_2), the inserts were removed, inverted to discard the medium, and gently rinsed twice with PBS. The cells were fixed with 4% paraformaldehyde for 30 min, rinsed, and stained with 0.1% crystal violet for another 30 min. After rinsing and air-drying, images were captured at 100× and 200× magnification (DMIL LED microscope) and analyzed using ImageJ software.

2.12. Western blot analysis

A pre-chilled radioimmunoprecipitation assay (RIPA) lysis solution, containing 1% phenylmethylsulfonyl fluoride (PMSF) and protease and phosphatase inhibitors, was used to lyse the cells. After 30 min on ice, the lysates were centrifuged at 12,000× g and 4 °C for 15 min. The supernatant was collected, and the BCA method was used to quantify protein concentration. Samples were diluted to equal concentrations, mixed with 5× SDS loading buffer, and denatured at 95 °C for 10 min. Equal amounts of protein (20–40 μg per lane) were loaded for SDS-PAGE electrophoresis at 80 V for the stacking gel and 120 V for the separating gel. Proteins were transferred to methanol-activated PVDF membranes using the wet transfer method (4 °C, 250 mA, 60–90 min). Membranes were blocked with (Tris-buffered saline with Tween 20) TBST containing 5% skim milk or BSA for 2 h. After TBST rinses, the membranes were incubated with horseradish peroxidase (HRP)-linked secondary antibodies for 1 to 2 h at room temperature. After an additional rinse, the protein signals were visualized using ECL, and images were recorded with a chemiluminescence detection system (5200, Tanon, China). Primary antibodies used included BAX (R013644, Epizyme), BCL-2 (A27315PM, Abclonal), MEK (R24949, Zenbio), ERK (A4782, Abclonal), p-PI3K (R27166, Zenbio), p-AKT (310021, Zenbio), and mTOR (A2445, Abclonal).

2.13. Statistical analysis

Each assay was performed in triplicate, and the results are reported as mean ± standard deviation. For comparisons involving more than two groups, data were analyzed by one-way ANOVA followed by Tukey's multiple comparison test, whereas two-tailed Student's *t*-tests were used for pairwise comparisons. A p-value < 0.05 was considered statistically significant. All statistical analyses were performed with GraphPad Prism 9.0, assuming parametric test conditions.

3. Results

3.1. Screening of targets for isorhamnetin and triple-negative breast cancer

The two-dimensional structure of ISO was obtained from the TCMSP database. Potential targets were predicted using SwissTarget Prediction (based on chemical similarity) and SuperPred (based on drug–target interaction signatures), yielding 100 and 109 targets, respectively. After integrating the predictions and standardizing target names using the UniProt database (official gene symbols), duplicates were removed, resulting in 198 unique potential targets of ISO. TNBC-associated therapeutic targets were collected from three authoritative disease databases: GeneCards (using a relevance score ≥10 as the inclusion threshold), OMIM (Online Mendelian Inheritance in Man, which catalogs known disease-associated genes), and DisGeNET (which integrates text mining and genome-wide association studies). After merging and deduplicating the three datasets, 1,490 potential TNBC targets were identified. The ISO target set and the TNBC target set were uploaded to the Venny 2.1 online platform for Venn diagram analysis to identify overlapping targets. Intersection analysis revealed 61 common targets between ISO and TNBC (Figure 1), suggesting that these targets may mediate the therapeutic effects of ISO against TNBC.

3.2. Protein–protein interaction network construction and core target analysis

For a clearer understanding of how the primary drug targets, disease processes, and signaling pathways are related, a protein–protein interaction network was constructed using the STRING database. High-confidence protein–protein interaction data were retrieved from STRING and loaded into Cytoscape for visualization and centrality analysis. Nodes were ranked by degree centrality, which reflects the number of direct connections each protein has in the network; a higher degree indicates a more prominent hub role. Using the NetworkAnalyzer plugin in Cytoscape, we calculated each node's degree centrality and identified 10 key targets: AKT1, heat shock protein 90 alpha family class A member 1 (HSP90AA1), EGFR, HIF-1α, SRC, NF-κB1, matrix metallopeptidase 9 (MMP9), poly (ADP-ribose) polymerase 1 (PARP1), glycogen synthase kinase 3 beta (GSK3β), and MCL1 (Figure 2). These core targets exhibit high connectivity in the protein–protein interaction network, suggesting they may play important regulatory roles in the action of ISO against TNBC.

3.3. Gene Ontology and Kyoto Encyclopedia of Genes and Genomes enrichment analyses

The intersection target set was imported into the DAVID database for enrichment analysis, resulting in 439 statistically significant GO terms ($p < 0.05$), including 278 biological process terms, 50 cellular component terms, and 111 molecular function terms. Terms were sorted by p-value, and the top 10 enriched terms in each category were selected to generate bubble plots (Figure 3). GO enrichment analysis showed that biological process terms were mainly related to ephrin receptor signaling, negative regulation of apoptotic processes, EGFR-associated receptor tyrosine kinase signaling, protein autophosphorylation, VEGF receptor-1-associated signaling, platelet-derived growth factor receptor alpha (PDGFRA) downstream signaling, and KIT signaling. Cellular component terms were mainly enriched in the nucleoplasm, nucleus, cytoplasmic matrix, protein complex, receptor complex, cytoplasm, intermediate filament, centrosome, mitochondria, and chromosomal telomere region. Molecular function terms were significantly enriched in ATP binding, protein phosphorylation catalysis, site-specific phosphorylation of histone H3 at Y41 and H2A.X at Y142, tyrosine-directed phosphorylation activity, kinase activity associated with collagen receptors, and macrophage colony-stimulating factor receptor binding/activation. KEGG pathway analysis indicated that the effects of ISO on breast cancer were closely related to the 20 most significant signaling pathways (adjusted p-value < 0.05), including EGFR tyrosine kinase

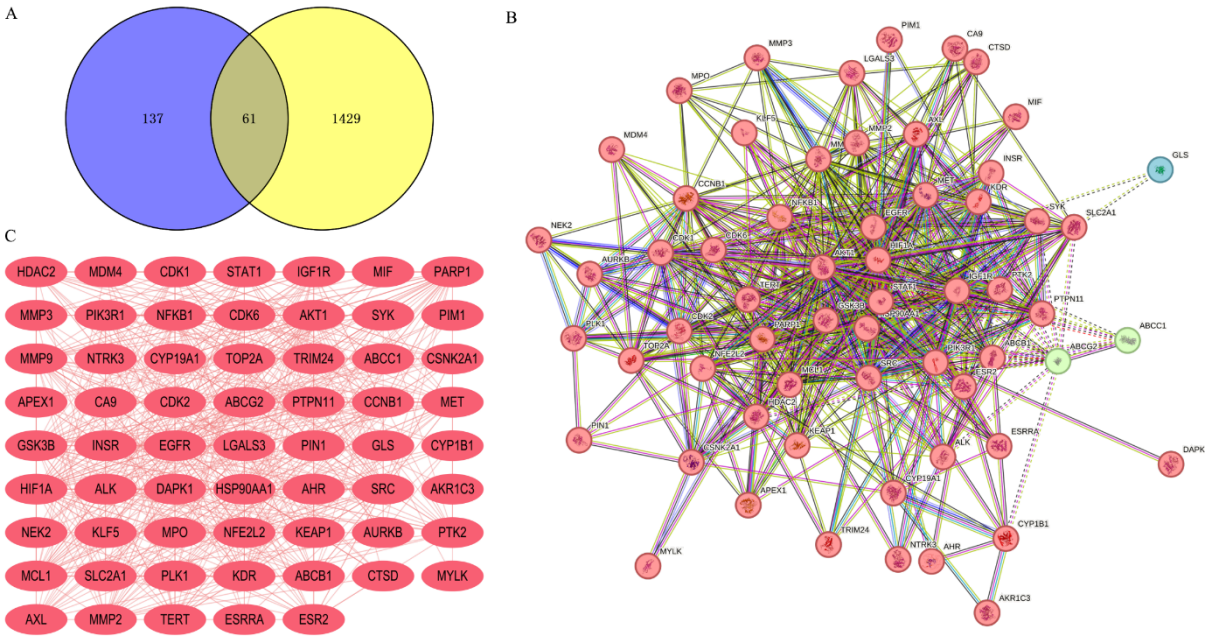

Figure 1. (A) Venn diagram of common targets between isorhamnetin and TNBC, and (B–C) the corresponding protein–protein interaction networks.

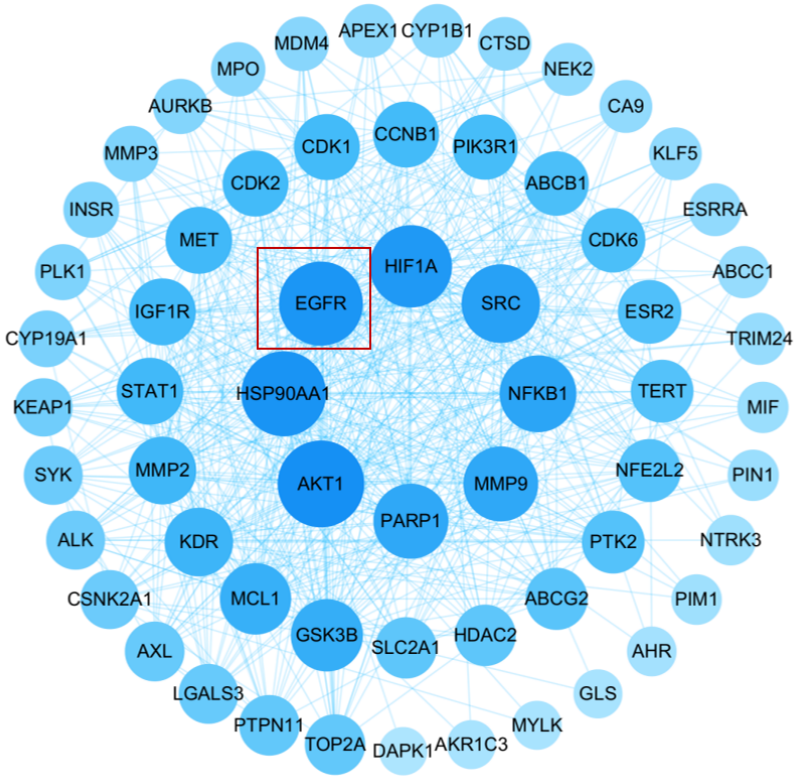

Figure 2. Protein–protein interaction network for the core targets shared between isorhamnetin and triple-negative breast cancer.

inhibitor (TKI) resistance, phosphoinositide 3-kinase (PI3K)–Akt signaling, programmed death-ligand 1 (PD-L1)/programmed cell death protein 1 (PD-1) checkpoint signaling, central carbon metabolism in cancer, estrogen signaling, HIF-1 signaling, thyroid hormone signaling, forkhead box O (FoxO) signaling, Ras signal transduction cascade, ErbB signaling, VEGF signaling, Janus kinase–signal transducer and activator of transcription (JAK–STAT) signaling, p53 signaling, and apoptosis (Figure 4).

3.4. Molecular docking

To assess possible direct binding between ISO and key human protein targets, molecular docking was performed with six proteins: EGFR, MCL1, MMP9, HIF-1α, PARP1, and MET. The docking results showed binding affinities of −5.975 kcal/mol for EGFR, −5.857 kcal/mol for MCL1, −5.430 kcal/mol for MMP9, −5.207 kcal/mol for HIF-1α, −4.814 kcal/mol for PARP1, and −4.721 kcal/mol for MET (Figure 5). According to conventional docking criteria, binding energies below −5.0 kcal/mol indicate relatively strong affinity, and more negative values indicate more stable binding. Based on this criterion, ISO showed strong binding to EGFR, MCL1, MMP9, and HIF-1α. Among these, EGFR had the lowest binding energy (−5.975 kcal/mol), suggesting the strongest affinity. Although the binding energies of PARP1 and MET were slightly above −5.0 kcal/mol, they still indicated moderate binding. Overall, the molecular docking results support EGFR as the most likely direct target of ISO.

3.5. Isorhamnetin inhibits triple-negative breast cancer cell proliferation

To evaluate the effect of ISO on the proliferative capacity of TNBC cells, a CCK-8 assay was used to determine IC50 values. The IC50 values were 38.99 μM for MDA-MB-231 cells and 35.80 μM for MDA-MB-468 cells. The cells were then treated with different concentrations of ISO (0, 10, 20, 40, and 80 μmol/L). The CCK-8 assay showed that ISO significantly inhibited the proliferative viability of both cell lines in a concentration- and time-dependent manner compared with the untreated control group (Figure 6B). The colony formation assay further validated the effect of ISO on long-term proliferative capacity. The two cell lines were seeded in six-well plates and treated with different concentrations of ISO (0, 10, 20, or 40 μM) for 10–14 days, followed by fixation, staining, and colony counting.

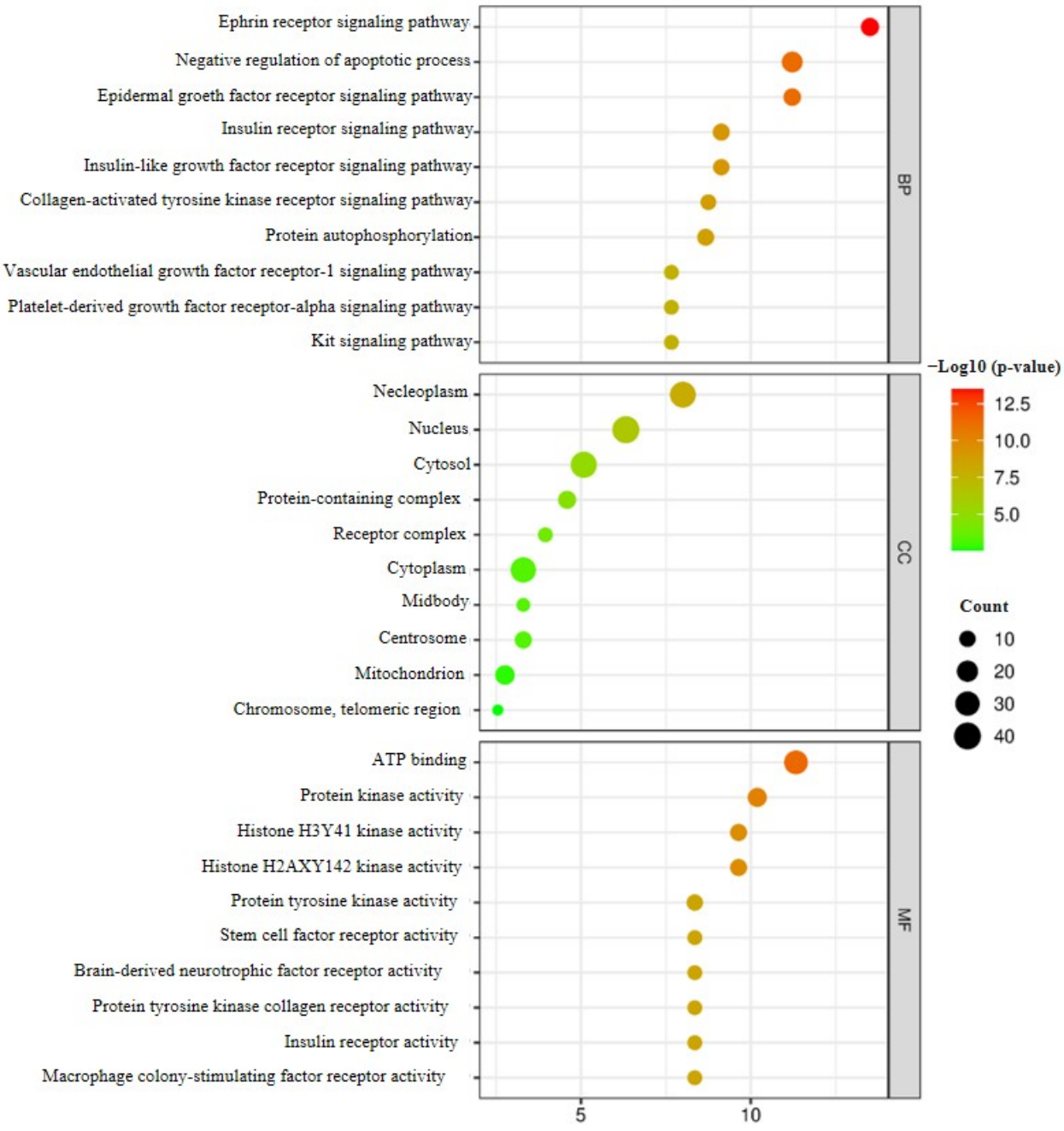

Figure 3. Gene Ontology enrichment analysis of the common targets shared between isorhamnetin and triple-negative breast cancer.

Compared with the control group, the number of colonies in the ISO-treated groups was significantly reduced in a concentration-dependent manner (Figure 6A, C, D).

3.6. Isorhamnetin inhibits triple-negative breast cancer cell migration and invasion

MDA-MB-468 and MDA-MB-231 breast cancer cells were maintained in logarithmic growth and then incubated with ISO. Cell migratory and invasive capacities were assessed using wound-healing and Transwell assays, respectively. The wound-healing assay showed that ISO significantly reduced the migration area of breast cancer cells (Figure 7A–C), indicating inhibition of cell migration. The Transwell assay showed that ISO decreased the number

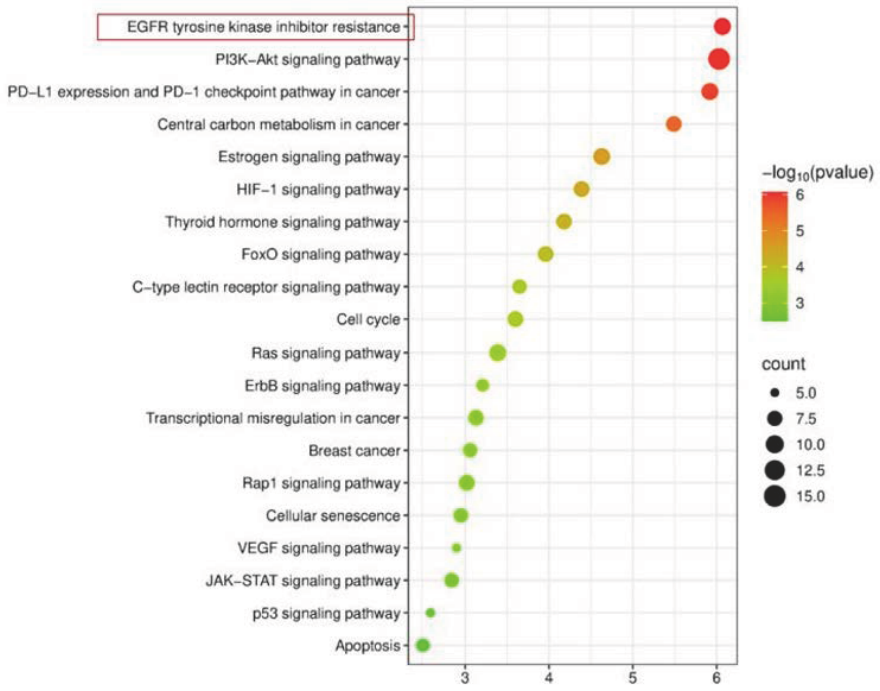

Figure 4. Kyoto Encyclopedia of Genes and Genomes enrichment analysis of the common targets shared between isorhamnetin and triple-negative breast cancer.

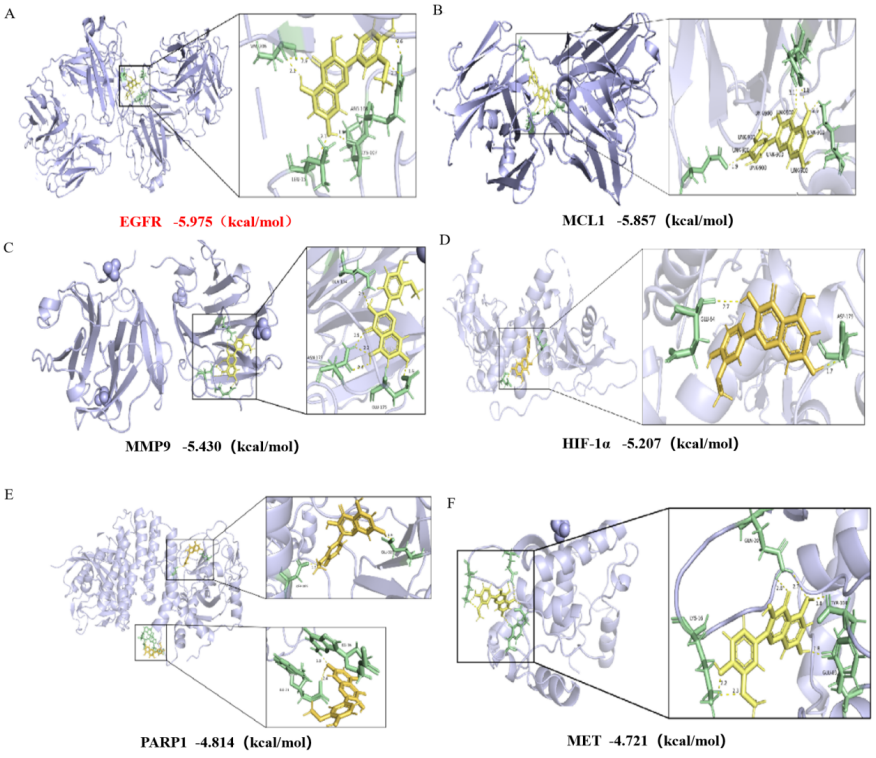

Figure 5. Molecular docking results of isorhamnetin (ISO) with core triple-negative breast cancer targets. Computational docking analyses of (A) ISO–epidermal growth factor receptor (EGFR) interaction, (B) ISO–MCL1 interaction, (C) ISO–matrix metallopeptidase (MMP9) interaction, (D) ISO–hypoxia-inducible factor 1 alpha (HIF-1α) interaction, (E) ISO–poly(ADP-ribose) polymerase 1 (PARP1) interaction, and (F) ISO–MET interaction.

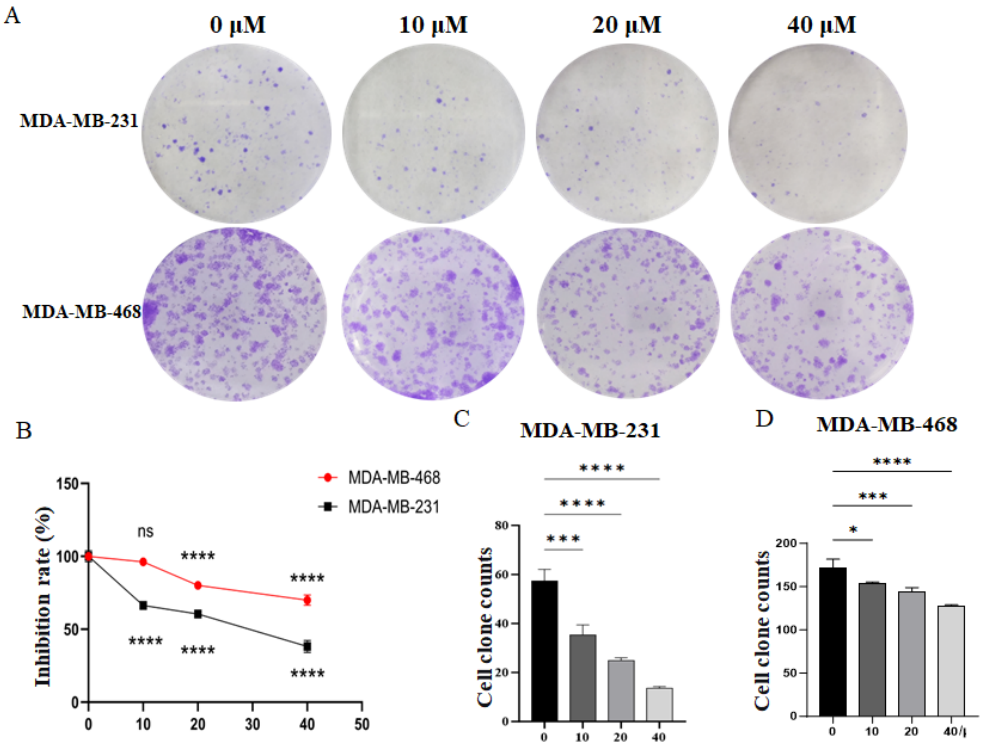

Figure 6. Isorhamnetin (ISO) inhibits the proliferation of triple-negative breast cancer cells. (A) Representative colony formation assay images. (B) Cell counting kit-8 assay results. (C, D) Quantitative analysis of colony numbers (n =3).
Notes: *p <0.05, ***p <0.001, ****p <0.0001).

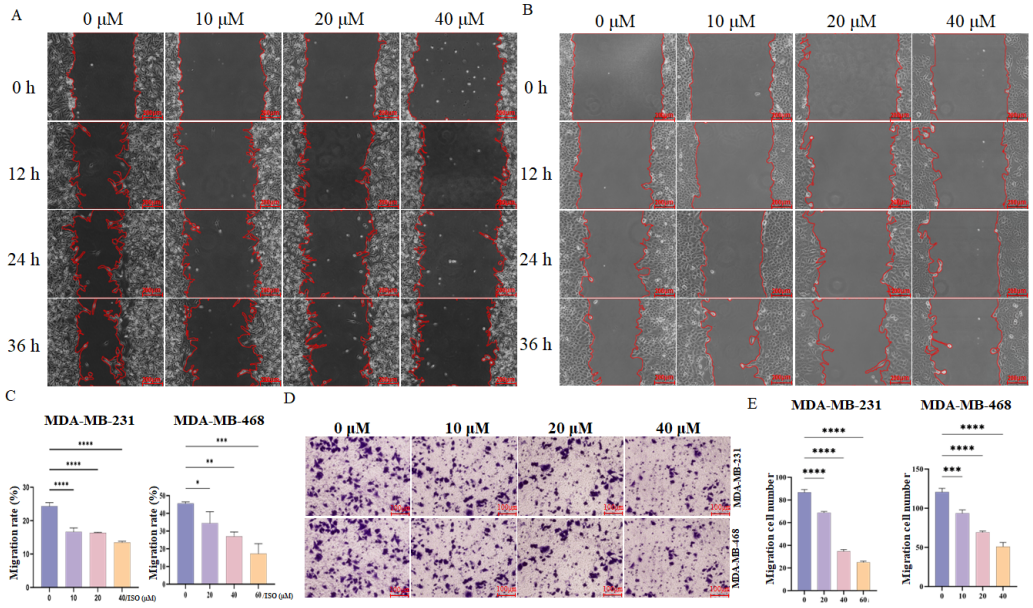

Figure 7. Isorhamnetin (ISO) inhibits the migration and invasion of triple-negative breast cancer cells. (A–B) Wound healing assay images of (A) MDA-MB-231 cells and (B) MDA-MB-468 cells. Scale bars: 200 μm; magnifications: 200×. (C) Quantitative analysis of the cell migration rate. (D) Transwell assay images of TNBC cells. Scale bars: 100 μm; magnifications: 200×. (E) Quantitative analysis of Transwell cell counts (n=3).
Notes: *p <0.05, **p <0.01, ***p <0.001, ****p <0.0001.

of cells invading from the upper chamber to the lower chamber, suggesting suppression of breast cancer cell invasion (Figure 7D, E).

3.7. Isorhamnetin enhances epidermal growth factor receptor thermal stability

To verify the direct binding between ISO and EGFR suggested by the docking results, a cellular thermal shift assay was performed in MDA-MB-231 and MDA-MB-468 cells (Figure 8A). The results showed that ISO significantly increased the thermal stability of EGFR in a temperature-dependent manner. Compared with the control group, the degradation temperature of EGFR in ISO-treated cells shifted to higher temperatures ($\Delta T_m > 2°C$), indicating that ISO directly binds to EGFR and stabilizes its structure against thermal denaturation (Figure 8B). These findings provide direct experimental evidence for a physical interaction between ISO and EGFR and support the molecular docking predictions.

3.8. Isorhamnetin targets EGFR and regulates mTOR and MEK/ERK signaling

To further elucidate the downstream signaling mechanisms through which ISO exerts its anti-TNBC effects, Western blot analysis was performed in MDA-MB-231 and MDA-MB-468 cells treated with ISO. The results showed that ISO significantly downregulated total EGFR protein in a dose-dependent manner. Moreover, the expression and phosphorylation levels of key downstream molecules in the PI3K/AKT/mTOR and MEK/ERK pathways were significantly reduced after ISO treatment (Figure 8C, D). These data indicate that ISO not only reduces EGFR expression but also inhibits activation of its downstream pro-survival and pro-proliferation signaling cascades. Collectively, these findings suggest that ISO suppresses TNBC cell malignancy by targeting EGFR and its downstream PI3K/AKT/mTOR and MEK/ERK signaling axes.

4. Discussion

This study integrated network pharmacology predictions, in silico docking studies, and cellular experiments to reveal the putative mechanisms underlying ISO-mediated inhibition of TNBC progression. The proliferative, motile, and invasive properties of MDA-MB-231 and MDA-MB-468 TNBC cells were significantly reduced by ISO treatment. The underlying mechanism may involve selective suppression of EGFR, as well as its downstream mTOR and MEK/ERK signal cascades.

Consistent with recent studies, our network pharmacology analysis further supported these findings. Recent studies suggest that network pharmacology can effectively predict common targets between traditional Chinese medicine or natural products and diseases, and identify key nodal proteins through protein–protein interaction networks.[28-30] In this study, this approach was used to screen 61 common targets between ISO and TNBC, among which EGFR, AKT1, HSP90AA1, and SRC occupied central positions in the protein–protein interaction network. Moreover, KEGG enrichment analysis showed that these molecular targets were mainly clustered in pathways closely related to oncogenesis, metastasis, and therapy resistance, including EGFR TKI resistance, PI3K–Akt, ErbB, HIF-1, and VEGF signaling. Our data indicate that ISO suppresses TNBC by acting on multiple targets and signaling pathways. This reflects the complexity of natural product action and highlights potential advantages over traditional single-target drugs.

Molecular docking results revealed a binding energy of −5.975 kcal/mol between ISO and EGFR, indicating strong binding affinity and suggesting that EGFR may be a potential direct target of ISO. This prediction was validated in a cellular thermal shift assay, where ISO treatment significantly enhanced the thermal stability of EGFR, providing classic evidence of direct binding between small molecules and target proteins. EGFR is often overexpressed or abnormally activated in various epithelial-derived tumors and is closely associated with tumor cell proliferation, invasion, and therapy resistance. In TNBC, approximately 50% of cases exhibit EGFR overexpression, and its expression level is correlated with poor prognosis.[31] Although the therapeutic efficacy of EGFR-targeted agents such as cetuximab and erlotinib in TNBC remains controversial, basic research suggests that EGFR inhibition can reverse epithelial-mesenchymal transition, enhance chemotherapy sensitivity, and suppress metastasis.[32] Therefore, targeting EGFR is a rational strategy for precision therapy in TNBC. This study is, to our knowledge, the first to suggest through combined computational and experimental approaches that ISO may directly act on EGFR.

Subsequent functional experiments demonstrated that ISO inhibited colony formation and the migration and invasion of TNBC cells, with effects increasing with drug concentration. Notably, abnormal EGFR activation can initiate multiple downstream signaling pathways, thereby promoting tumor progression.[33,34] Among these, the PI3K/Akt/mTOR and MEK/ERK pathways are the two most classic pro-survival and pro-proliferation signaling axes downstream of EGFR, and their abnormal activation jointly drives malignant tumor phenotypes.[35-37] Western blot analysis further showed that ISO treatment reduced

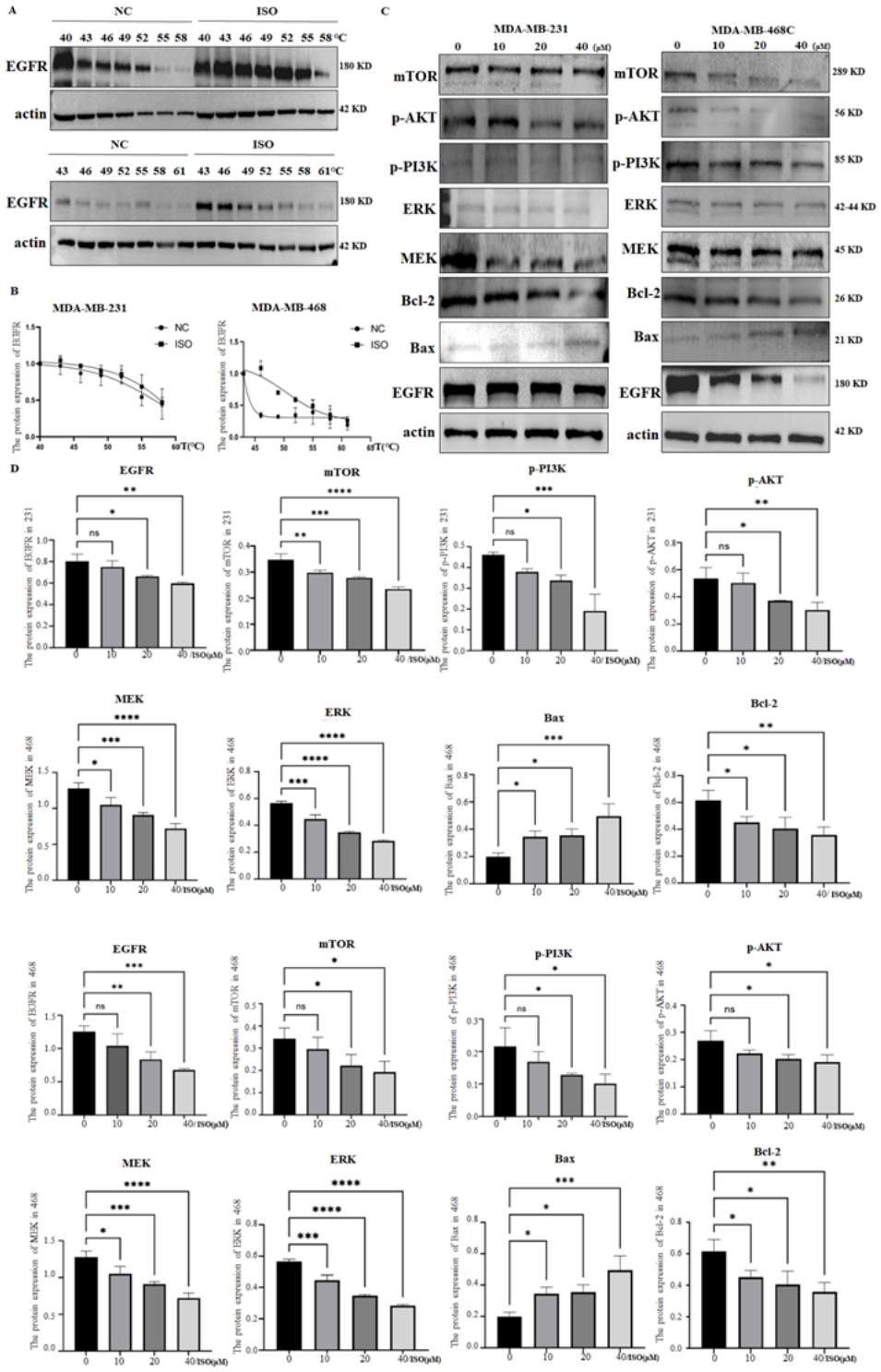

Figure 8. Isorhamnetin (ISO) targets epidermal growth factor receptor (EGFR) and regulates the mammalian target of rapamycin (mTOR) and MAPK/ERK kinase (MEK)/extracellular signal-regulated kinase (ERK) signaling pathways. (A, B) ISO enhanced the thermal stability of the EGFR protein, as demonstrated by the cellular thermal shift assay. (C) Western blot analysis of EGFR, mTOR, phosphoinositide 3-kinase (PI3K), AKT, MEK, BAX, and B-cell lymphoma 2 (BCL-2) expression. (D) Quantitative analysis of protein band intensity. (n =3).
Notes: *p <0.05, **p <0.01, ***p <0.001, ****p <0.0001.
Abbreviation: NC: Negative control.

total EGFR protein expression while simultaneously inhibiting the phosphorylation levels of key downstream signaling nodes in the PI3K/Akt/mTOR and MEK/ERK pathways. These changes are consistent with suppression of the EGFR signaling axis, suggesting that targeting the upstream receptor EGFR may allow ISO to inhibit multiple downstream oncogenic signals simultaneously, potentially avoiding compensatory activation from single-pathway inhibition and thereby enhancing anti-tumor effects while delaying drug resistance.

Several limitations should be noted. First, only cell-based assays were performed; therefore, further studies are needed to evaluate the anti-tumor efficacy, pharmacokinetics, and safety of ISO in rodent TNBC models. Although existing studies suggest that ISO can arrest the cell cycle and promote tumor cell apoptosis, its in vivo efficacy and optimal dosing regimen in specific TNBC subtypes remain to be clarified.[38,39] Future studies should evaluate ISO in orthotopic TNBC mouse models, perform pharmacokinetic profiling to determine optimal dosing, and use surface plasmon resonance or competitive binding assays to quantify the binding affinity between ISO and EGFR. The potential synergistic effects of ISO with conventional chemotherapeutics, such as paclitaxel, also merit investigation. Finally, the specific contributions of other core targets predicted by network pharmacology, such as AKT1 and HIF-1α, to the anti-TNBC effects of ISO, as well as their interactions with the EGFR signaling network, require further investigation. Recent studies also suggest that AKT1 may be a key direct target of ISO,[40,41] and its regulatory mechanisms in TNBC warrant further in-depth research.

In summary, this study suggests that the natural flavonoid compound ISO may directly target EGFR and inhibit its downstream PI3K/AKT/mTOR and MEK/ERK signaling axes, thereby suppressing the malignant phenotypes of TNBC cells in vitro. Because a systematic comparison across cell lines with different EGFR expression levels was not conducted, it remains unclear whether these effects are EGFR-dependent and require further investigation. These findings provide experimental evidence that may help clarify how ISO acts against breast cancer, while also establishing a basis for its future use as an inhibitor of EGFR signaling. They may also inform clinical studies exploring ISO as a potential primary or adjunctive treatment for TNBC. Future work should focus on in vivo validation, deeper mechanistic studies, and formulation optimization to support translation into clinical applications.

5. Conclusion

This study preliminarily suggests that ISO may inhibit the progression of malignant phenotypes in TNBC cells in vitro, potentially by targeting EGFR and its downstream mTOR/MEK–ERK signaling pathways. This finding provides preliminary experimental evidence for ISO as a potential natural candidate for TNBC.

Acknowledgments

None.

Funding

This work was supported by the National Natural Science Foundation of China (Grant number 82505697).

Conflict of interest

The authors declare no conflict of interest.

Author contributions

Conceptualization: Yanan Hua
Formal analysis: Yanan Hua
Investigation: Xiangyu Xie
Methodology: Li Sun
Visualization: Enqi Liu
Writing–original draft: Xiangyu Xie
Writing–review & editing: Yanan Hua, Shuqi Niu

Ethics approval and consent to participate

Not applicable.

Consent for publication

Not applicable.

Availability of data

All data and materials generated or analyzed during this study are included in this published article.

References

1. Xiong X, Zheng LW, Ding Y, *et al*. Breast cancer: pathogenesis and treatments. *Signal Transduct Target Ther*. 2025;10(1):49.

   doi: 10.1038/s41392-024-02108-4

2. Juan C, Peng Y. The Molecular Landscape and Utility of Multiomic Analyses in Triple-Negative Breast Cancer: Further Subtyping and Exploring Novel Biomarkers and Therapeutic Targets. *Cancers (Basel)*. 2025;1(24):4003.

   doi: 10.3390/cancers17244003

3. Zhang HP, Jiang RY, Zhu JY, *et al*. PI3K/AKT/mTOR signaling pathway: an important driver and therapeutic

target in triple-negative breast cancer. *Breast Cancer*. 2024;31(4):539-551.

doi: 10.1007/s12282-024-01567-5

4. Khan N, Jabeen S. Evaluation of the Clinical Impact of Immune Checkpoint Inhibitors (Atezolizumab and Pembrolizumab) in the Treatment of Triple-Negative Breast Cancer: A Meta-Analysis and Review of Literature. *Cureus*. 2025;17(12):e98330.

doi: 10.7759/cureus.98330

5. Gao X, Han Y, Yang L, *et al*. Harmonizing yin and yang, remodeling the microenvironment: the adjuvant potential of Chinese herbal medicine in tumor immunotherapy. *Front Oncol*. 2026;16:1806602.

doi: 10.3389/fonc.2026.1806602

6. Li X, Wang L, Ni B, Wang J, Sun YF. Research Progress of Natural Compounds from Chinese Herbal Medicine in the Treatment of Melanoma. *Curr Treat Options Oncol*. 2025;26(7):533-568.

doi: 10.1007/s11864-025-01322-8

7. Kushwaha PP, Singh AK, Prajapati KS, *et al*. Induction of apoptosis in breast cancer cells by naphthylisoquinoline alkaloids. *Toxicol Appl Pharm*. 2020;409:115297.

doi: 10.1016/j.taap.2020.115297

8. Sahoo S, Mohapatra P, Sahoo SK. Flavonoids for the treatment of breast cancer, present status and future prospective. *Anticancer Agents Med Chem*. 2023;23(6):658-675.

doi: 10.2174/1871520623666221024114521

9. Ateba SB, Mvondo MA, Ngeu ST, *et al*. Natural terpenoids against female breast cancer: a 5-year recent research. *Curr Med Chem*. 2018;25(27):3162-3213.

doi: 10.2174/0929867325666180214110932

10. Singh S, Verma R. Exploring the Therapeutic Potential of Flavonoids in the Management of Cancer. *Curr Pharm Biotechnol*. 2025;26(1):17-47.

doi: 10.2174/0113892010297456240327062614

11. Cheng X, Tan S, Duan F, Yuan QQ, Li QR, Deng G. Icariin induces apoptosis by suppressing autophagy in tamoxifen-resistant breast cancer cell line MCF-7/TAM. *Breast Cancer*. 2019;26(6):766-775.

doi: 10.1007/s12282-019-00980-5

12. Paramanantham A, Kim MJ, Jung EJ, *et al*. Pretreatment of anthocyanin from the fruit of *vitis coignetiae* pulliat acts as a potent inhibitor of TNF-α effect by inhibiting NF-κB-regulated genes in human breast cancer cells. *Molecules*. 2020;25(10):2396.

doi: 10.3390/molecules25102396

13. Luan YY, Liu ZM, Zhong JY, Yao RY, Yu HS. Effect of grape seed proanthocyanidins on tumor vasculogenic mimicry in human triple-negative breast cancer cells. *Asian Pac J Cancer Prev*. 2015;16(2):531-535.

doi: 10.7314/apjcp.2015.16.2.531

14. Shricastava S, Jeengar MK, Thummuri D, *et al*. Cardamonin, a chalcone, inhibits human triple negative breast cancer cell invasiveness by downregulation of Wnt/β-catenin signaling cascades and reversal of epithelial-mesenchymal transition. *Biofactors*. 2017;43(2):152-169.

doi: 10.1002/biof.1315

15. Shi K, Li X, Chen R, Shi BK, Wang K, Zhu YF. Bousigonine D from *Bousigonia mekongensis* inhibits bladder cancer growth and overcomes cisplatin resistance. *Sci Rep*. 2025;15(1):16254.

doi: 10.1038/s41598-025-96892-w

16. Bi Q, Wang M, Luo L, *et al*. Wenxia Changfu Formula inhibits NSCLC metastasis by halting TAMs-induced epithelial-mesenchymal transition via antagonistically modulating CCL18. *Chin J Nat Med*. 2025;23(7):838-847.

doi: 10.1016/S1875-5364(25)60912-5

17. Ma S, Li J, Hao B, Fan L. Current status of traditional Chinese medicine in modulating mitochondrial metabolic abnormalities in tumors. *Cancer Biol Med*. 2025;22(12):1439-1454.

doi: 10.20892/j.issn.2095-3941.2025.0246

18. Park C, Cha HJ, Choi EO, *et al*. Isorhamnetin Induces Cell Cycle Arrest and Apoptosis Via Reactive Oxygen Species-Mediated AMP-Activated Protein Kinase Signaling Pathway Activation in Human Bladder Cancer Cells. *Cancers*. 2019;11(10):1494.

doi: 10.3390/cancers11101494

19. Luo W, Liu Q, Jiang N, Li MQ, Shi L. Isorhamnetin inhibited migration and invasion via suppression of Akt/ERK-mediated epithelial-to-mesenchymal transition (EMT) in A549 human non-small-cell lung cancer cells. *Biosci Rep*. 2019;39(9):BSR20190159.

doi: 10.1042/BSR20190159

20. Mei C, Zhang X, Zhi Y, *et al*. Isorhamnetin Regulates Programmed Death Ligand-1 Expression by Suppressing the EGFR–STAT3 Signaling Pathway in Canine Mammary Tumors. *Int J Mol Sci*. 2024;25(1):670.

doi: 10.3390/ijms25010670

21. Kim S, You D, Jeong Y, *et al*. Berberine down-regulates IL-8 expression through inhibition of the EGFR/MEK/ERK pathway in triple-negative breast cancer cells. *Phytomedicine*. 2018;50:43-49.

doi: 10.1016/j.phymed.2018.08.004

22. He JY, Huang ZR, Han LZ, Gong Y, Xie CH. Mechanisms and management of 3rd-generation EGFR-TKI resistance in

advanced non-small cell lung cancer (Review). *Int J Oncol*. 2021;59(5):90.

doi: 10.3892/ijo.2021.5270

23. Dai S, Liu YT, Liu ZR, *et al*. Cancer-associated fibroblasts mediate resistance to anti-EGFR therapies in cancer. *Pharmacol Res*. 2024;206:107304.

doi: 10.1016/j.phrs.2024.107304

24. Tardito S, Matis S, Zocchi MR, Benelli R, Poggi A. Epidermal Growth Factor Receptor Targeting in Colorectal Carcinoma: Antibodies and Patient-Derived Organoids as a Smart Model to Study Therapy Resistance. *Int J Mol Sci*. 2024;25(13):7131.

doi: 10.3390/ijms25137131

25. Cui NP, Qiao S, Jiang S, *et al*. Protein Tyrosine Kinase 7 Regulates EGFR/Akt Signaling Pathway and Correlates With Malignant Progression in Triple-Negative Breast Cancer. *Front Oncol*. 2021;11:699889.

doi: 10.3389/fonc.2021.699889

26. Mei C, Liu Y, Liu ZY, *et al*. Dysregulated Signaling Pathways in Canine Mammary Tumor and Human Triple Negative Breast Cancer: Advances and Potential Therapeutic Targets. *Int J Mol Sci*. 2024,26(1):145.

doi: 10.3390/ijms26010145

27. Tang AH, Hoefer RA, Guye ML, Bear HD. Persistent EGFR/K-RAS/SIAH pathway activation drives chemo-resistance and early tumor relapse in triple-negative breast cancer. *Cancer Drug Resistance*. 2022;5(3):691-702.

doi: 10.20517/cdr.2022.31

28. Yang LF, Wang HY, Zhu ZY, *et al*. Network Pharmacology-Driven Sustainability: AI and Multi-Omics Synergy for Drug Discovery in Traditional Chinese Medicine. *Pharmaceuticals (Basel)*. 2025;18(7):1074.

doi: 10.3390/ph18071074

29. Mangral ZA, Bhat BA, Sheikh S, *et al*. Exploring the therapeutic potential of *Rhododendron anthopogon* D.Don essential oil constituents against lung cancer: A network pharmacology-based analysis with molecular docking and experimental studies. *Comput Biol Med*. 2025;187:109827.

doi: 10.1016/j.compbiomed.2025.109827

30. Li XB, Li XD, Wang L, *et al*. Advancing Traditional Chinese Medicine Research through Network Pharmacology: Strategies for Target Identification, Mechanism Elucidation and Innovative Therapeutic Applications. *Am J Chin Med*. 2025;53(7):2021-2042.

doi: 10.1142/S0192415X25500752

31. Ilie SM, Briot N, Constatin G, *et al*. Pathologic and immunohistochemical prognostic markers in residual triple-negative breast cancer after neoadjuvant chemotherapy. *Front Oncol*. 2024;13:1309890.

doi: 10.3389/fonc.2023.1309890

32. An XL, Xie J, Wang WY, Long T, Liang QH, Hou J. Why does EGFR-targeted therapy continue to fail in breast cancer? From mechanistic deciphering to novel intervention strategies. *Crit Rev Oncol Hematol*. 2026;220:105186.

doi: 10.1016/j.critrevonc.2026.105186

33. Ganesan K, Xu C, Du B, *et al*. Isoliquiritigenin: A natural compound with a promising role in inhibiting breast cancer lung metastasis. *J Tradit Complement Med*. 2025;15(7):702-713.

doi: 10.1016/j.jtcme.2024.10.001

34. Kim ES. Molecular targets and therapies associated with poor prognosis of triple-negative breast cancer (Review). *Int J Oncol*. 2025;66(6):52.

doi: 10.3892/ijo.2025.5758

35. Panda VK, Mishra B, Swain B, *et al*. Molecular Insights on Signaling Cascades in Breast Cancer: A Comprehensive Review. *Cancers (Basel)*. 2025;17(2):234.

doi: 10.3390/cancers17020234

36. Abizadeh E, Berglas E, Abizadeh A, *et al*. Current and Emerging Therapies for Targeting the ERK1/2 & PI3K Pathways in Cancer. *Int J Mol Sci*. 2025;26(17):8696.

doi: 10.3390/ijms26178696

37. Shahiwala A. Convergent and Divergent Signaling Pathways in Cancer: A Dual-Axis Model for Adaptive Precision Oncology. *Oncology*. 2025;39(9):386-393.

doi: 10.46883/2025.25921052

38. Duan SH, Li XY, Song CL, *et al*. Isoliquiritigenin Inhibits Triple-Negative Breast Cancer Progression via Targeting the IRF5/SLC7A5/IDO1-Mediated Tryptophan Metabolism Pathway. *Oncol Res*. 2025;33(11):3543-3556.

doi: 10.32604/or.2025.068292

39. Tang SW, Deng ZQ, Ou MJ, Wang ZX. Pharmacological Potentials and Delivery Strategies of Isoliquiritigenin: Challenges and Advances in Enhancing Bioavailability. *Drug Des Devel Ther*. 2025;19:9879-9911.

doi: 10.2147/DDDT.S534713

40. Sharma D, Dhobi M, Lather V, Pandita D. An insight into the therapeutic effects of isoliquiritigenin in breast cancer. *Naunyn Schmiedebergs Arch Pharmacol*. 2024;397(12):9503-9519.

doi: 10.1007/s00210-024-03282-6

41. Xue Y, Wang MJ. Isoliquiritigenin in Breast Cancer: A Systematic Review of Its Preventive and Anti-metastatic Mechanisms. *Iran J Pharm Res*. 2025;24(1):e165301.

doi: 10.5812/ijpr-165301